Journal of Soils and Sediments
https://doi.org/10.1007/s11368-021-02997-w

SOILS, SEC 4 • ECOTOXICOLOGY • RESEARCH ARTICLE

Durability analysis of bio-cemented slope soil under the exposure of acid rain

Sivakumar Gowthaman[1] · **Kazunori Nakashima**[1] · **Satoru Kawasaki**[1]

Received: 22 December 2020 / Accepted: 1 June 2021

Abstract

Purpose Instability of slope surface is a critical concern in Geotechnical and Environmental Engineering. MICP (Microbial-Induced Carbonate Precipitation), an innovative bio-cementation technique, has attracted the attention for slope surface protection. In this work, MICP was investigated to evaluate its durability under the exposure of acid rain and to advance the understanding on long-term performance of slope soil preserved by MICP.

Methods MICP treatment was applied to a fine-grained slope soil using indigenous bacteria. Specimens treated to different cementation levels (% $CaCO_3$) were exposed to acid rain (of varying pH) through two sorts of mechanisms: (i) infiltration and (ii) immersion. The evaluations were based on corrosion of $CaCO_3$, mass loss, needle penetration tests, and scanning electron microscopy.

Results The decrease in pH increased the corrosion of $CaCO_3$, resulting in considerable loss in aggregate and unconfined compressive strength. However, increased cementation level showed high durability of specimens. The soils treated to 12.5% $CaCO_3$ showed 19.9% soil loss, whereas it was reduced to 5.4% when cemented to 22.5% $CaCO_3$. The results also revealed that the contact time of acid rain significantly governed the rate of corrosion, i.e., specimens subjected to lower infiltration rate (20 mm/h) showed higher loss of mass compared to that of higher rate (100 mm/h).

Conclusion The long-term performance of MICP treatment is determined by (i) cementation level, (ii) pH, and (iii) infiltration rate of acid rain. High cementation level promotes the longevity of the treatment. Therefore, MICP to higher cementation level is recommended for long-term preservation of slope surface.

Keywords Microbial-induced carbonate precipitation (MICP) · Slope surface · Preservation · Durability · Long-term performance · Cementation level

1 Introduction

Microbial-induced carbonate precipitation (MICP) is a novel bio-cementation technique, which has gained an increased attention among geotechnical researchers (DeJong et al. 2010; Achal and Mukherjee 2015; Tang et al. 2020). MICP is an environmentally friendly process that mediates non-pathogenic bacteria containing active urease enzymes. During the method, the bacteria are aerobically cultivated and introduced to the target soil along with the solution of urea and calcium chloride. When the urea molecules are exposed to bacterial enzymes, ureolysis takes place immediately, resulting in the formation of carbonate and ammonium ions in the aqueous media (Eq. 1). Meanwhile, in the presence of calcium ions, the calcium carbonate (cementing agent) is precipitated into the soil matrix (Eq. 2). The bacteria cells which are attached to the soil particles provide nucleation to calcium carbonate being precipitated, leading the crystals to grow from the surface and to create the bridges with adjacent surfaces (Burbank et al. 2013). The intergranular cementation has been shown to significantly enhance the geotechnical engineering properties of soils including shear strength parameters (Nafisi et al. 2020; Gowthaman et al. 2020), stiffness (Montoya and De Jong 2015), and dilative characteristics (Lin et al. 2016; Feng and Montoya 2017).

Responsible editor: Dong-Mei Zhou

✉ Sivakumar Gowthaman
gowtham1012@outlook.com

[1] Faculty of Engineering, Hokkaido University, Sapporo 060-8628, Japan

Published online: 11 June 2021

$$H_2N - CO - NH_2 + 2H_2O \xrightarrow{\text{urease}} CO_3^{2-} + 2NH_4^+ \quad (1)$$

$$Ca^{2+} + CO_3^{2-} \rightarrow CaCO_3(s) \downarrow \quad (2)$$

It is evident that the MICP treatment desirably transitions the soil from loose state to aggregated state (i.e., soft rock-like material) (Montoya and De Jong 2015), indicating that the bonding of soil particles by calcium carbonate decreases the likelihood of particle mobility and detachability. Consequently, MICP is drawing more attentions these days for stabilizing slope surface. Recent studies evidenced that MICP technique could promote the cover condition of the slope, providing a marked increase in stability of surface substrates against various slope degradation processes. For example, the enhancement in scouring resistance of MICP treated foreshore slopes was demonstrated under simulated tidal waves (Salifu et al. 2016; Bao et al. 2017; Liu et al. 2020). Jiang et al. (2019) assessed the erodibility under rainfall effects, suggesting that treatment by 1 mol/L cementation media could provide better erosion resistance among 0.2–2 mol/L. Chung et al. (2020) studied the responses of MICP-treated slope under varying rainfall intensities (13.5, 33 and 75 mm/h) and gradients (5.1°, 8.5°, and 15°), demonstrating that soil loss was more influenced by the intensity compared to the slope gradient. Recently, Gowthaman et al. (2020) deployed the MICP to slope soil and investigated the durability under cyclic freeze–thaw effects. Their results indicated that the aggregate stability is primarily attributed to the content of calcium carbonate which resists the crystal-soil ruptures and detachments during the frost of pore water.

Among the varying environmental factors, acid rain is one of the most serious concerns worldwide. The industrial activities had a great role in atmospheric acidification, i.e., the emission of sulfur and nitrogen oxides (SO_x and NO_x) results in the formation of strong sulfuric and nitric acids in atmospheric water, leading to the formation of detrimental acid rain (Grennfelt et al. 2020). It has often been documented that the acid rain causes chemical deterioration and detrimental effects in soils (Kamon et al. 1997; Bakhshipour et al. 2016). Particularly, carbonate-rich geomaterials (e.g., limestone, sandstone, calcareous sand) undergo dissolution when exposed to acid rain, resulting in deterioration on their geotechnical stability (Basu et al. 2020). However, the destruction time scale of a geomaterial was found to be reliant on either chemical characteristics of acid rain or that of geomaterials (Teir et al. 2006; Li et al. 2019). In MICP treatment, the stabilization of slope surface is the result of soil particles bonded by calcium carbonate, and which would possibly undergo a progressive impairment under exposure to acid rain.

Recently, Chen and Achal (2020) observed the persistence of precipitated calcium carbonate under varying pH levels (3.5–7.0), ensuring that the MICP treatment can be durable under acid rain environment. Most of the existing studies evaluated the strength deterioration of MICP-treated sands by fully immersing them into acid solution, suggesting that the chemical condition of the solution governs the corrosion of $CaCO_3$ (Liu et al. 2019; Wei et al. 2019). However, the real scenario of the slope surface would be different, because the water-logged/immersed condition seldom occurs near the surface (Harden and Scruggs 2003; Muntohar and Liao 2010). The precipitated flux of acid rain would either infiltrate through MICP-treated surface or flow over the surface, rather the immersion. Therefore, in order to effectively design the MICP treatment, it is necessary to understand how the infiltration process and intensity of the flux interact with MICP-treated surface. Besides, it is worth noting that the effect of cementation level (% $CaCO_3$) and how the level impacts on durability under prolonged exposure of acid rain has not been studied so far.

In Hokkaido (the northmost island of Japan), the engineering problems caused by acid rainfall is more prominent since several decades ago. Therefore, a deeper understanding on durability responses of MICP treatment under the exposure of acid rain is essential prior to the in situ applications. For the above purpose, slope soil treated to different levels (12–23% $CaCO_3$) was subjected to acid rain (of varying pH levels 3.0–6.0) in the laboratory through two possible mechanisms (infiltration and immersion). For the infiltration case, the effect of two supply intensities (20 mm/h and 100 mm/h) was studied. The evaluation program was based on corrosion of $CaCO_3$, mass loss, needle penetration tests, and scanning electron microscopy (SEM), and the results are discussed in detail.

2 Material and methods

2.1 Soil properties

One of the erosion-prone expressway slopes located in Do-O expressway line of Hokkaido (Japan) was chosen for the investigation as the representative. For the experiments, disturbed soil samples were obtained at the site (42.388532 N; 140.284762E) (refer to Fig. S1 in supplementary material), sealed in plastic bags and transported to the laboratory. The stratigraphy of the slope was found to consist of fine sand and silt; the grain size distribution is shown in Fig. 1. Based on the Unified Soil Classification System (USCS) (ASTM 2017), the soil can be classified as poorly graded sand (SP). Results of chemical analysis performed using energy dispersive X-ray fluorescence (XRF) spectrometer (JSX-3100R II JOEL, Japan) verified that the soil primarily consisted of SiO_2, Al_2O_3, and Fe_2O_3 of around 58%, 26%, and 9%, respectively.

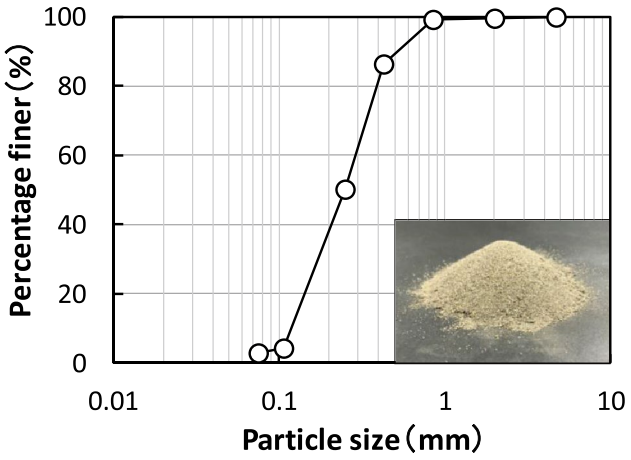

Fig. 1 Grain size distribution curve of the slope soil

2.2 Bacteria and growth media

The ureolytic bacteria *Lysinibacillus xylanilyticus* (designated DSM 23,493) isolated by Gowthaman et al. (2019a) from the above target slope was used in this study due to its reliable ureolytic performance and non-pathogenicity (bio-safety level: 1). The ATCC 1376 medium (consisted of 10 g/L ammonium sulfate, 20 g/L yeast extract and 15.7 g/L tris buffer) was used to grow the bacteria. Inoculated bacteria culture was subjected to shaking incubation at 25 °C and 160 rpm. When the colonies were fully grown, i.e., when the optical density at 600 nm (OD_{600}) reached to around 4.0 (after 72 h), the bacteria culture was harvested for soil treatment. The urease activity of the bacteria culture, measured by indophenol spectrophotometry, was around 2.7 ± 0.6 mM urea hydrolyzed/minute at 25 °C, and the enzymatic performance of the bacteria was relatively consistent for 7 days.

2.3 Preparation and MICP treatment

In this preliminary study, column specimens were used to evaluate the durability responses of MICP-treated slope surface. During preparation, cylindrical molds (inner diameter of 30 mm) were positioned vertically, and the soil was packed (50 mm height) to the average dry density in the range of 1.5 ± 0.05 g/cm^3. All the specimens were then placed into the incubator of 25 °C, followed by the MICP treatment. Following the methods suggested in previous works (Martinez et al. 2013; Cheng and Cord-Ruwisch 2014), a two-phase treatment was performed. The prepared bacteria culture of 10 mL was applied in the first phase. After 2 h of immobilization time, similar quantity of cementation media (consisted of 111 g/L $CaCl_2$, 60 g/L urea and 6 g/L nutrient broth) was applied in the subsequent phase. Both the bacteria solution and cementation media were simply introduced on the surface and allowed to percolate the columns under gravitational and capillary effects. During the treatment, cementation media was applied to the soil every 24 h. As the effective performance of bacteria is typically limited to 7–8 days, bacteria culture was needed to be applied once again after 7 days of treatment.

To achieve different levels of cementation (w/w % of precipitated $CaCO_3$), different durations of treatment were undertaken. In this study, the specimens were treated to three average cementation levels (in the range of 12–23% of $CaCO_3$ by weight), which literally fall under heavy cementation category (Feng and Montoya 2016). As the aggregate stability was the major concern for enhancing the surface condition of the slope, the heavy cementation category was desirably chosen for the investigation. Accordingly, the specimens were percolated by 7, 10, and 14 numbers of cementation media, and the average cementations of 12–13%, 17–18%, and 22–23% of $CaCO_3$ were achieved, respectively. The calcium carbonate content was determined using the acid reaction method, and the methodology is discussed in subsequent section. By the end of the treatment process, the specimens were rinsed adequately by using tap water in order to eliminate the unreacted salts and chemicals. Afterward, the molds were cut, and the specimens were carefully taken out. Finally, each specimen was trimmed smoothly to the height of 30 mm, followed by subjected to acid rain simulation test as described subsequently. The physical appearance of the MICP treated specimens is shown in Fig. 2a.

2.4 Acid rain solution

Atmospheric water, owing to the dissolution of CO_2, reveals the pH value in a range between 5.6 and 7.0 (Xie et al. 2004; Teir et al. 2006). When the sulfur and nitrogen oxides get contact with atmospheric water, acidification occurs, which leads the pH of acid rain to often fall in a range between 3.0 and 6.0 (Kamon et al. 1997; Bakhshipour et al. 2016; Chen and Achal 2020), and the pH below 3.0 was reported to hardly occur (Teir et al. 2006). Therefore, considering the possible situations, the acid rain used in this study was prepared at three different pH conditions (6.0 ± 0.1, 4.5 ± 0.1, and 3.0 ± 0.1) by equally dropping high concentrated H_2SO_4 and HNO_3 acids into deionized distilled water. It is worth noting that the pH of rainfall in study area (Hokkaido, Japan) was recorded between 4.4 and 5.6 as per the past 30 years of meteorological data (1990–2019).

2.5 Acid rain simulation test

To study the durability, the MICP-treated soils were subjected to acid rain through two possible mechanisms: (i) infiltration and (ii) immersion. The infiltration test was performed according to the procedure documented in Bakhshipour et al. (2016). As shown in Fig. 2b, the MICP

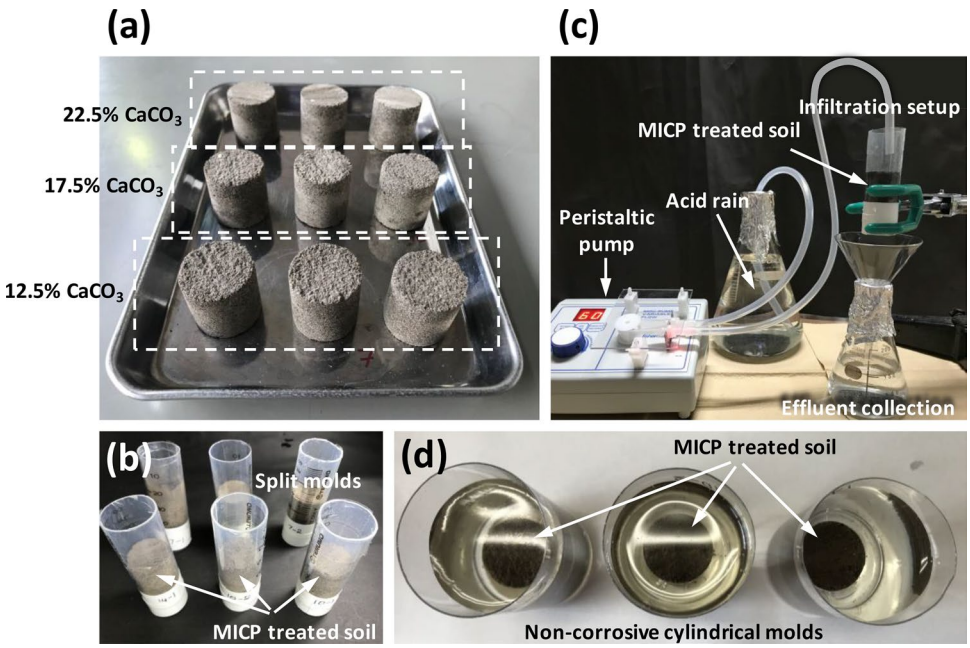

Fig. 2 **(a)** Appearance of the MICP treated soil specimens of varying treatment levels, **(b)** specimens prepared in split-cylinders for infiltration tests, **(c)** infiltration test set up and **(d)** immersion test arrangement

specimens were prudently placed and confined within split-cylinders (non-corrosive) with 30 mm internal diameter and 70 mm height, and a membrane gauze was placed at the bottom of the cylinders. Figure 2c shows the set up fabricated for the infiltration test. Using a peristaltic pump, the acid rain solution was supplied at uniform rates to the infiltration cell. Two rates of supply were tested herein for infiltration, mimicking high and low intensities of acid rain (100 mm/h and 20 mm/h, respectively). Each specimen was infiltrated to the total acid rain volume of 4.5 L (equivalent to the precipitation of 15 years), and during the process, the effluent was collected (every 0.1 L in separate beaker) and subjected to chemical analysis. In total, eighteen specimens were tested, and the test conditions corresponding to the infiltration are summarized in Table 1.

The immersion test was performed in accordance with the methods suggested in previous works (Xie et al. 2004; Liu et al. 2019). The detail of the specimens used for immersion test is given in Table 2. As presented in Fig. 2d, each specimen was fully submerged into separate non-corrosive cylindrical containers (60 mm in diameter and 70 mm in height) filled with 0.1 L acid rain solution. As the H^+ ions were consumed by $CaCO_3$ material, the pH of the acid rain solution would increase with the immersion time; therefore, the acid rain solution was replaced with freshly prepared solution of 0.1 L every 24 h, and the specimens were submerged to the total duration of 45 days (total acid rain volume of 4.5 L per specimen).

During the treatment, a batch of control specimens was also prepared simultaneously in order to compare the impacts of acid rain on the properties of MICP-treated specimens. The as-treated characteristics of those specimens were evaluated without subjecting to acid rain, and the details of the control specimens are presented in Table 3.

2.6 Evaluation program

The evaluation program mainly consisted of the following: (i) measurement of Ca^{2+} ions (LAQUA-twin calcium meter, HORIBA Advanced Techno Co., Ltd.), (ii) soil loss, (iii) needle penetration tests, and (iv) scanning electron microscopy (SEM) analysis. The unconfined compressive strength (UCS) of the specimens was determined using needle penetration test in accordance with the standard of Japanese Geotechnical Society (JGS 2012). During the test, the needle attached to the device (SH-70, Maruto Testing Machine Company, Tokyo) was penetrated into the specimen; meanwhile, the penetration depth (mm) of the needle and the penetration resistance (N) were directly measured from the penetrometer. Using the regression relationship (Eq. 3) developed by analyzing 50 cemented soil samples, the UCS of the specimen was estimated, where x is penetration gradient (ratio between penetration resistance (N) and penetration depth (mm)); y is the corresponding UCS:

$$\log(y) = 0.978\log(x) + 2.621 \quad (3)$$

$CaCO_3$ content (also referred to as cementation level) of MICP-treated slope soil was determined by using a simplified device developed by Fukue et al. (1999) to measure the pressure of carbon dioxide released when the MICP-treated specimen was reacted with 2 mol/L concentrated HCl in closed system under constant volume and temperature. Initially, the mass of the oven-dried (105 °C for 48 h) sample

Table 1 Detail of specimens used for acid rain tests by infiltration

Test category	Specimen designation	Number of MICP treatment	Supply rate of acid rain	Acidity level (pH)	Total flux
[a]Infiltration	HI-7–1	7	100 mm/h	6.0 ± 0.1	4.5 L
	HI-7–2	7	100 mm/h	4.5 ± 0.1	4.5 L
	HI-7–3	7	100 mm/h	3.0 ± 0.1	4.5 L
	HI-10–1	10	100 mm/h	6.0 ± 0.1	4.5 L
	HI-10–2	10	100 mm/h	4.5 ± 0.1	4.5 L
	HI-10–3	10	100 mm/h	3.0 ± 0.1	4.5 L
	HI-14–1	14	100 mm/h	6.0 ± 0.1	4.5 L
	HI-14–2	14	100 mm/h	4.5 ± 0.1	4.5 L
	HI-14–3	14	100 mm/h	3.0 ± 0.1	4.5 L
[b]Infiltration	LI-7–1	7	20 mm/ h	6.0 ± 0.1	4.5 L
	LI-7–2	7	20 mm/h	4.5 ± 0.1	4.5 L
	LI-7–3	7	20 mm/h	3.0 ± 0.1	4.5 L
	LI-10–1	10	20 mm/h	6.0 ± 0.1	4.5 L
	LI-10–2	10	20 mm/h	4.5 ± 0.1	4.5 L
	LI-10–3	10	20 mm/h	3.0 ± 0.1	4.5 L
	LI-14–1	14	20 mm/h	6.0 ± 0.1	4.5 L
	LI-14–2	14	20 mm/h	4.5 ± 0.1	4.5 L
	LI-14–3	14	20 mm/h	3.0 ± 0.1	4.5 L

[a]Specimens were infiltrated at acid rain supply of 100 mm/h, simulating high intensity rainfall

[b]Specimens were infiltrated at the supply of 20 mm/h, simulating low intensity rainfall

was measured, and the sample was placed into the system. Subsequently, the vials filled with HCl were carefully set into the system without spattering the specimen. The system was finally closed, and the HCl was allowed to react with the specimen until the connected manometer read a constant pressure value. Using the calibration curve developed between $CaCO_3$ and pressure, the weight of the $CaCO_3$ was estimated, and $CaCO_3$ content (%) was determined according to the Eq. 4:

$$CaCO_3 \text{ content } (\%) = \frac{\text{Weight of } CaCO_3}{\text{Weight of the oven dried specimen} - \text{Weight of } CaCO_3} \quad (4)$$

To observe the microstructure of the MICP-treated specimens, SEM analysis was performed using Miniscope TM 3000 (Hitachi, Tokyo, Japan). The representative samples were carefully cored from the samples and observed through SEM after the oven dry at 60 °C for 24 h.

2.7 Statistical analysis

The experimental results were analyzed using R Statistical Package (version 4.0.3) to determine the significance of differences between the means of experimental sets obtained herein. The P value less than 0.05 (i.e., $P < 0.05$) was considered as the significance range.

Table 2 Detail of specimens used for acid rain tests by immersion

Test category	Specimen designation	Number of MICP treatment	Acidity level (pH)	Duration of immersion
Immersion (fully submerged)	FS-7–1	7	6.0 ± 0.1	45 days
	FS-7–2	7	4.5 ± 0.1	45 days
	FS-7–3	7	3.0 ± 0.1	45 days
	FS-10–1	10	6.0 ± 0.1	45 days
	FS-10–2	10	4.5 ± 0.1	45 days
	FS-10–3	10	3.0 ± 0.1	45 days
	FS-14–1	14	6.0 ± 0.1	45 days
	FS-14–2	14	4.5 ± 0.1	45 days
	FS-14–3	14	3.0 ± 0.1	45 days

Table 3 Detail of the prepared control specimens

Specimen designation	Number of cementation treatment	[a]Spatial distribution of $CaCO_3$ (%)			
		Top	Middle	Bottom	Average
C-7–1	7	14.1	12.8	10.7	12.5
C-7–2	7	14.7	13.2	9.9	12.6
C-7–3	7	13.2	12.4	11.2	12.3
C-10–1	10	19.8	17.9	16.2	18.0
C-10–2	10	18.2	17.0	15.7	17.0
C-10–3	10	20.1	17.4	14.9	17.5
C-14–1	14	24.7	22.7	19.6	22.3
C-14–2	14	25.2	22.0	20.5	22.6
C-14–3	14	26.2	21.9	19.3	22.5

[a]Control specimens were divided into three evenly spaced sections along the height of the specimen (defined as top, middle and bottom), and the calcium carbonate contents were separately measured

3 Results

3.1 Corrosion of calcium carbonate

Throughout the test, the concentration of calcium ions (Ca^{2+}) was continually measured in the solution (for every 100 mL), and the quantity of corroded Ca^{2+} of each case is plotted against acid rain volume in Fig. 3. It can be seen that in all the cases, the corrosion of Ca^{2+} appears to linearly increase with the increasing acid rain volume. Higher rates of corrosion are evidenced in the specimens subjected to lower pH conditions. pH 3.0 cases showed obviously the sharp increase in the graphs (Fig. 3a–c), followed by pH 4.5 (Fig. 3d–f) and then pH 6.0 (Fig. 3g–i) (the respective mean corrosion rates were 1.25 ± 0.22, 0.38 ± 0.08, and 0.03 ± 0.01 μmol Ca^{2+}/mL). This could be attributed to the increased concentration of protons (H^+) in acid rain solution of low pH level (Xie et al. 2004; Teir et al. 2006). As

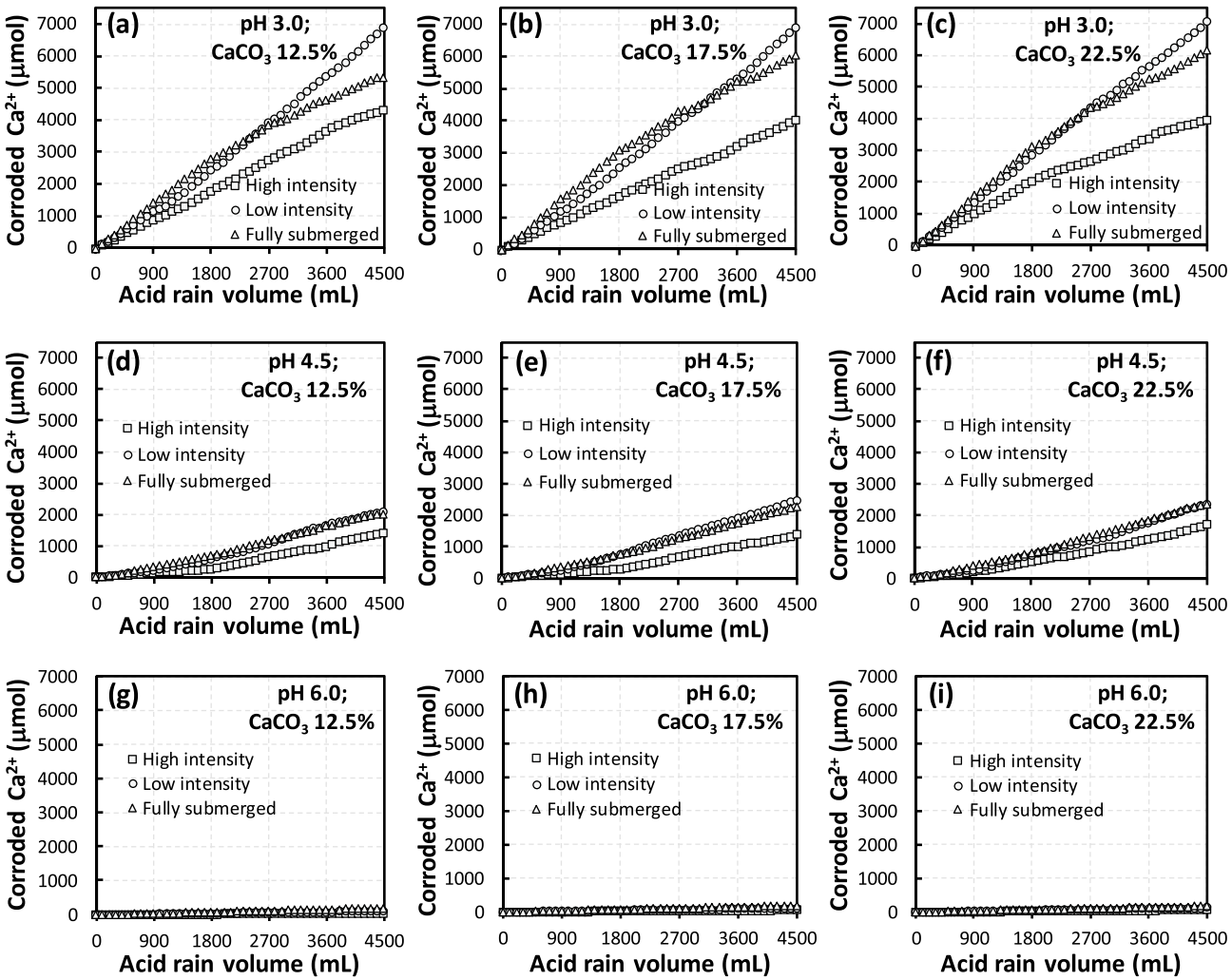

Fig. 3 Corroded calcium ions measured during the acid rain test (results of all the test cases are presented separately)

shown in the reactions (Eqs. 5–7), the oxonium ions (H_3O^+) formed from the acids (sulfuric and nitric acids) react with calcium carbonate crystals, turning them into lattice ions and CO_2 gas. Therefore, more or less of the H^+ concentration would in turn increase or decrease the reaction and dissolution of $CaCO_3$ molecules, respectively. The measured pH in reacted solutions was observed to be in a range of 6.5–8.0 (refer Fig. S2 of supplementary document), indicating that the dissolution of $CaCO_3$ would consume the protons and neutralize the acid rain solution. Similar pH values in effluent were also reported by Cheng et al. (2013) when MICP treated sand exposed to acid rain (pH 3.5).

$$H^+ + H_2O \leftrightarrow H_3O^+ \tag{5}$$

$$CaCO_3 + H_3O^+ \rightarrow Ca^{2+} + CO_3^{2-} + H_2O \tag{6}$$

$$H_2CO_3 \leftrightarrow CO_2 + H_2O \tag{7}$$

From Fig. 3, it can also be observed that the delivery of acid rain solution had a considerable impact in corrosion rate. The specimens which were infiltrated at high intensity (supply rate of 100 mm/h) exhibit low rate of Ca^{2+} corrosion (0.95 ± 0.04 µmol Ca^{2+}/mL at pH 3.0), whereas it was quite high when they were infiltrated at low intensity (20 mm/h) of acid rain solution (1.51 ± 0.05 µmol Ca^{2+}/ mL at pH 3.0). For a clear explanation, total corroded calcium carbonate at the end of the test was theoretically estimated in each case (from Ca^{2+} measurements), and the comparison is presented in Fig. 4. As seen, the corrosions of $CaCO_3$ at 20 mm/h delivery rate are around 1.7, 1.6, and 1.9 times higher than those at 100 mm/h at pH 3.0, 4.5, and 6.0, respectively. Statistical analysis revealed that the comparison yielded a significant difference at all the pH conditions ($P = 0.0004$, 0.003, and 0.0003, respectively). Relatively, a similar tendency is witnessed in all the cementation levels. This can possibly be explained by the effect of contact time. At high supply rate, the solution tended to infiltrate rapidly, which led the solution to have less contact time within specimen, resulting in less reaction with $CaCO_3$. On the other hand, the low supply rate facilitated relatively slow infiltration, allowing sufficient time to the reaction with $CaCO_3$ during the percolation. Moreover, the corrosion of calcium carbonate observed in fully submerged case is rather similar to that of 20 mm/h delivery.

3.2 Mass loss and physical changes

After every 900 mL of acid rain delivery, the specimens were prudently rinsed by distilled water and oven dried at 60 °C for 48 h, followed by the measurement of weight loss. Figure 5 presents the mass loss of MICP treated specimens as a function of volume of acid rain. The observed increase

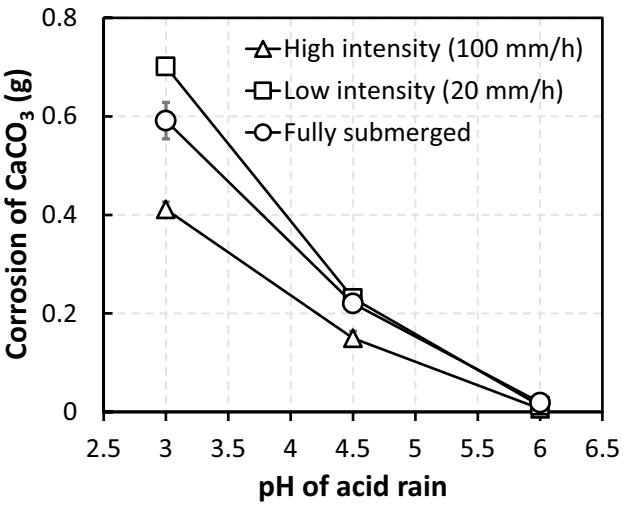

Fig. 4 Total corroded calcium carbonate versus pH of the acid rain (the vertical error bars represent mean ± SD of specimens ($n = 3$) tested for each condition)

in loss with increasing immersion volume of acid rain could be attributed to the progressive dissolution of $CaCO_3$. At low pH level (pH 3.0), owing to the high concentration of protons, the dissolution of $CaCO_3$ was high and led to the rapid destruction of connection/ bond between soil particles. As the result, specimens immersed into acid rain of pH 3.0 exhibited higher rates of aggregate loss compared to that at pH 4.5 and 6.0. For example, the rates of aggregate loss for 12.5% $CaCO_3$ specimens were 1.4×10^{-3} g/mL, 9.8×10^{-4} g/mL, and 2.7×10^{-4} g/mL at pH 3.0, 4.5, and 6.0, respectively.

It is interesting to mention that the cementation level (% $CaCO_3$) is more likely to have a great impact on loss of MICP-treated slope soil. As observed previously (in Fig. 3), the corrosion of calcium was found not to be influenced by the cementation level of MICP specimen; the corrosion values were pretty much similar in all the cementation levels at a specific pH condition. However, the results in Fig. 5 indicate that the mass loss is not influenced by pH alone, but also by the cementation level. The mass loss data plotted against the cementation level are shown in Fig. 6, clearly demonstrating that the loss decreases with the increase in cementation level, regardless of the conditions tested. For instance, when subjected to 20 mm/h acid rain delivery of pH 3.0, the evaluated mass losses were 19.9%, 8.8%, and 5.6% for the specimens treated to $CaCO_3$ levels of 12.5%, 17.5%, and 22.5%. In another term, the rates of soil loss were 1.4×10^{-3} g/mL, 6.5×10^{-4} g/mL, and 4.2×10^{-4} g/mL, while the corresponding corrosions of $CaCO_3$ were pretty similar (0.69 g, 0.69 g, and 0.71 g, respectively). Similar effect could also be witnessed in other pH as well as delivery conditions (Fig. 6).

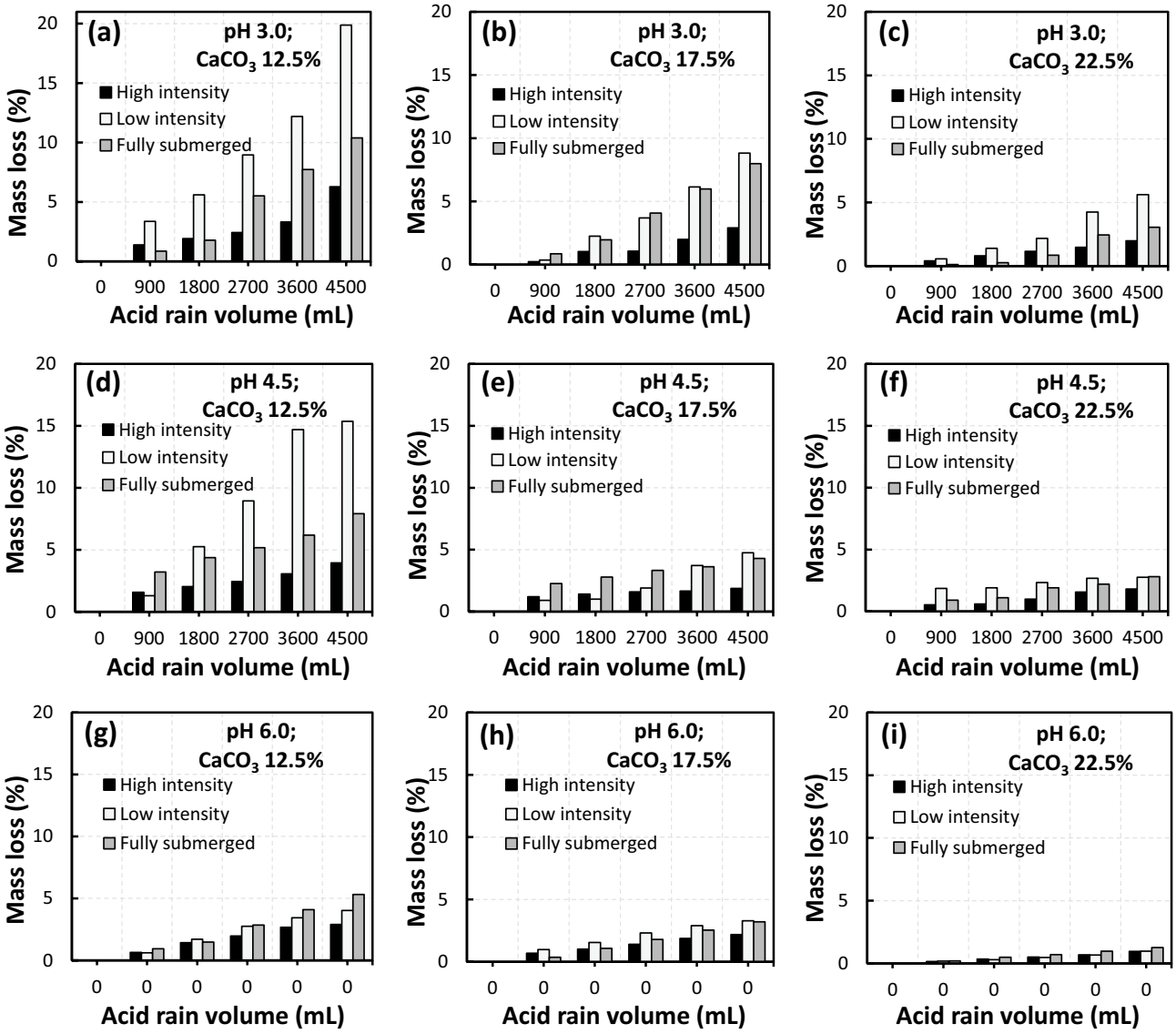

Fig. 5 Mass loss as a function of acid rain volume (results of all the test cases are presented separately)

When the test was progressed, considerable physical changes were observable in MICP-treated specimens. The damages were able to seen quite early in specimens tested by acid rain of pH 3.0; soil particles were observed to be detached rapidly from the specimen. On the other hand, only a minor damage was witnessed for the specimens tested using acid rain of pH 6.0. It should be noted that the specimens which were subjected to infiltration exhibited more impairment at the top part, but the bottom specimens remained relatively undamaged. Because, during the infiltration, the specimen's top (closest to supply point) was exposed to significantly more H^+ than the bottom, which led to more destruction of carbonate bonds at the top. But, as depicted in Fig. 7, the damages could be witnessed all over the specimen surface when subjected to immersion. It could also be seen that the specimens treated to 22.5% $CaCO_3$ reveled a negligible physical damage and could preserve its initial skeleton throughout the test.

3.3 Mechanical properties of specimens exposed to acid rain

To explore the change in mechanical properties of MICP-treated slope soil, specimens exposed to acid rain were tested for UCS, and the results were compared with the control specimens. Figure S3 (refer supplementary material) shows the comparison of UCS of the specimens subjected to different acid rain tests. As seen, the values after subjected to acid rain are observably lower than that of control ones (analysis revealed that the means are statistically significant ($P < 0.05$)

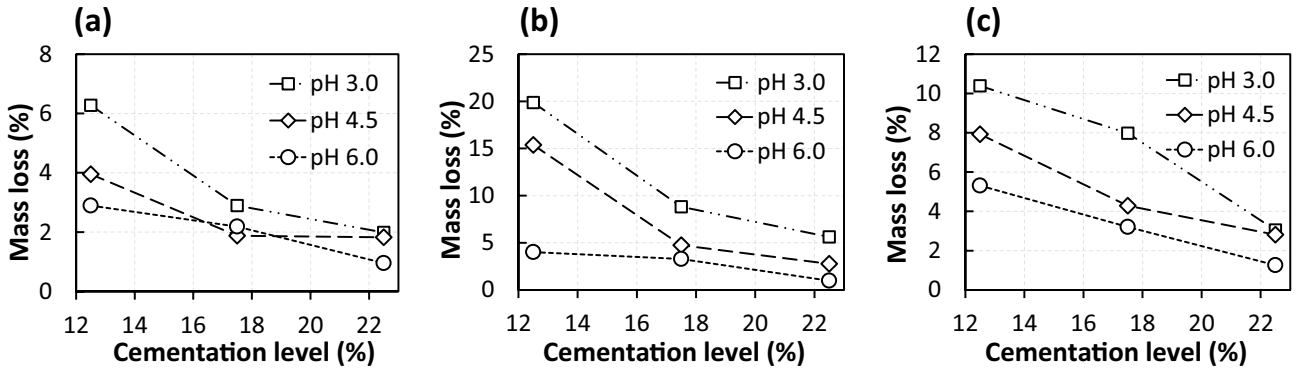

Fig. 6 The mass loss during acid rain test plotted against cementation level for the (**a**) infiltration (100 mm/h), (**b**) infiltration (20 mm/h), and (**c**) immersion cases

in all the cases). In all the test conditions, lower pH condition resulted in higher drop in UCS, which is consistent with many previous works (Li et al. 2019; Liu et al. 2019). For example, when the specimens (12.5% $CaCO_3$) were exposed to high-intensity infiltration, average UCS persists at 79.8%, 40.5%, and 36.1% relative to that of control specimen for the cases of pH 6.0, 4.5, and 3.0, respectively. The observation also reveals that the increase in cementation level appears to hold relatively higher UCS compared to that of low content of calcium carbonate.

4 Discussion

4.1 Effect of cementation level on durability

Previous studies showed that the strength and stability of the MICP-treated aggregates are immensely governed by the calcium carbonate formed within the voids (van Paassen et al. 2010; Lin et al. 2016; Cui et al. 2017). Figure 8 presents the microscale characteristics of the MICP-treated slope soil with different magnifications before subjected to acid rain test (control specimen). It can be observed that the calcite clusters that crystallized at particle contacts could enable the connectivity between soil particles, contributing as the primary source for strength and stability. Similar morphology of the calcium carbonate mineral could also be witnessed in other MICP-related works (Zhang et al. 2017; Omoregie et al. 2019). Moreover, there are crystals which were formed randomly on soil surfaces without subsidizing interparticle connection; by reducing the void spaces, however, those could secondarily contribute to the strength of the matrix (DeJong et al. 2010).

When the MICP-treated soil encounters the acid rain solution, the corrosion of calcium carbonate occurs, which appear to destroy the particle aggregation. The SEM images of specimens after the exposure of acid rain are shown in Fig. 9. It can be found that the effect of acid rain on the fabric of 12.5% $CaCO_3$ specimen is more intense compared to that of 22.5% $CaCO_3$. Comparing the changes in microstructure of control (Fig. 8) and 12.5% $CaCO_3$ case (Fig. 9a, b), it can be observed that the calcite clusters were significantly corroded, and the interparticle connections appear to be almost abolished. The prints of soil particles detached from the cementation could also be witnessed in micrographs along with residues of $CaCO_3$. On the other hand, the microstructure of 22.5% $CaCO_3$ specimens (Fig. 9c, d) could partly hold the original microstructure. Although the specimen underwent similar corrosion, the shape of the calcite clusters is quite similar to that observed in control specimen, and the interparticle connections are found to be better persisting compared to that observed in 12.5% $CaCO_3$.

For instance, the soil particles detached from the specimens during the test were collected and observed by SEM, and the observations are shown in Fig. 9e, f. Most of the detached particles were likely to be the same as untreated soils, whereas $CaCO_3$ residues were barely observed, as

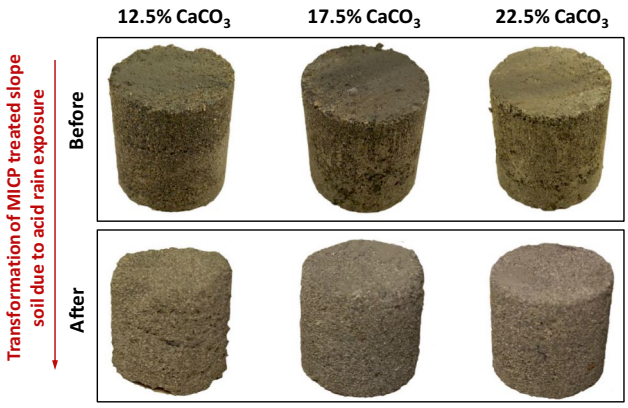

Fig. 7 Physical appearance of specimens after subjected to acid rain test (Note: the specimens belong to immersion test category of pH 3.0)

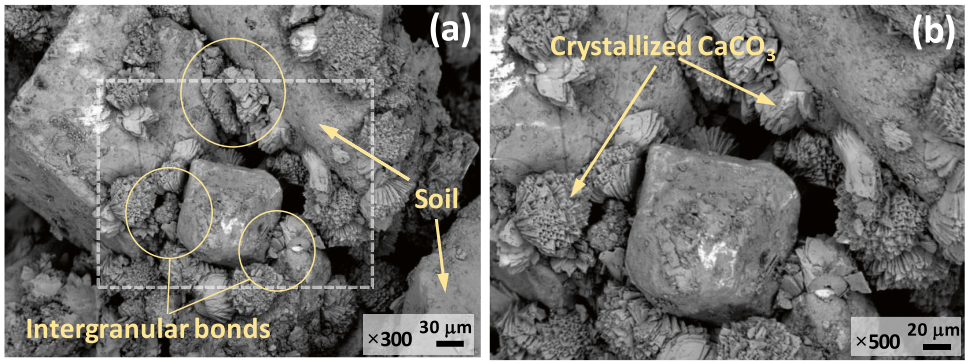

Fig. 8 SEM images of MICP treated slope soil before subjected to acid rain: **(a)** magnification of × 300 and **(b)** magnification of × 500 (Note: SEM images are of specimens treated to 22.5% $CaCO_3$)

specified in Fig. 9f. Basically, the detachability of a soil particle from the aggregation is mainly governed by the bonding strength at the contact point (Gowthaman et al. 2020). In the case of 22.5% $CaCO_3$, the soil particles are cemented by high content of calcium carbonate (i.e., formation of larger clusters with large contact area) at contacts, yet the cementation content was comparatively low in the case of 12.5% $CaCO_3$.

It was found that the dissolution rate of $CaCO_3$ depends mainly on the conditions of acid rain exposed (Fig. 3). However, the durability of the MICP treated soil is found not to be reliant on the pH alone. As graphically explained

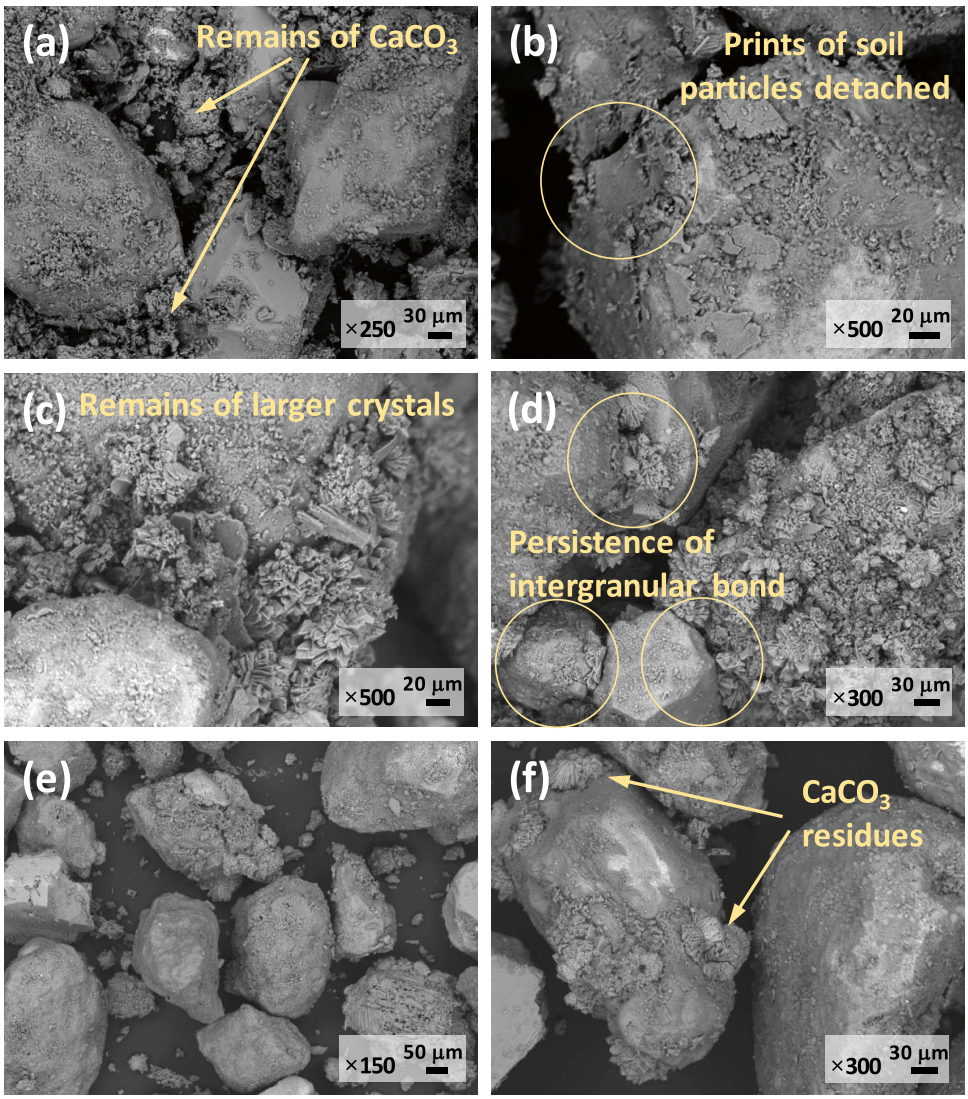

Fig. 9 SEM images of MICP treated slope soil after subjected to acid rain test: (**a**, **b**) specimens treated to 12.5% $CaCO_3$, (**c**, **d**) specimens treated to 22.5% $CaCO_3$, and (**e**, **f**) soil particles detached from the specimens (Note: the specimens used for SEM were tested under same acid rain conditions, pH 3.0)

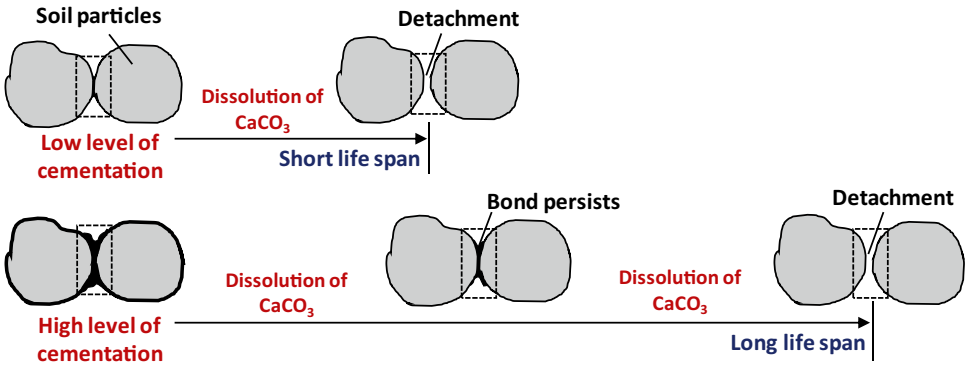

Fig. 10 Conceptually illustrating the effect of cementation level on the longevity of the MICP treatment under the exposure to acid rain

in Fig. 10, if the specimens are treated to higher levels of $CaCO_3$, the dissolution of bridges would require longer exposure of acid rain. It is quite the opposite, if the specimens are treated to lower levels of $CaCO_3$; the dissolution would be achieved with the shorter exposure, suggesting that the more or less of the precipitation content at particle contact would in turn increase or decrease the longevity of the treatment, respectively.

4.2 Effect of acid rain conditions on durability

The results of this study showed that the corrosion rate of $CaCO_3$ is determined by mainly two factors: (i) the pH condition and (ii) the contact time of acid rain (Fig. 4). Decrease in pH of the acid rain is found to accelerate the corrosion process, and this finding agrees with the results found in many previous works (Xie et al. 2004; Liu et al. 2019). In addition to the pH, the chemical composition of acid rain was reported to have considerable influence in corrosion process. It was previously found that sulfuric acid is more aggressive than nitric acid (Eyssautier-Chuine et al. 2016); thus, the increase in the sulfuric acid content in acid rain can be expected to result in increased corrosion compared to the nitric acid. However, a recent study could evidence that a skin of partially soluble calcium sulfate precipitates when MICP-treated sand reacts with sulfuric acid, providing supplementary strength and extending the durability of sand (Li et al. 2019). It should be noted that in this study, the formation of calcium sulfate was not encountered, which was confirmed by XRD analysis (Fig. S4 of supplementary material) performed to the specimens subjected to acid rain test. The morphology of the crystal which existed before and after the acid rain test was found to be only calcite.

In this study, it has also been found that the intensity of acid rain impacts on contact/reaction time of acid rain-$CaCO_3$. With increasing intensity of acid rain (comparing 100 mm/h and 20 mm/h), corrosion rate showed a decreasing trend (Figs. 3, 4). This finding would be significant to understand and evaluate the corrosion process in field scale. In other terms, for a same rainfall record, the corrosion would vary depending on the intensity of the acid rainfall. During heavy rainfall, the flux that either flow over the surface or rapidly infiltrate into the slope would have less impact on MICP-treated surface in terms of contact time and corrosion. On the contrary, the mild and prolonged rainfalls are more likely to be detrimental to the surface, because the slow infiltration of the flux enables increased reaction with carbonates, leading to severe damage as witnessed in this work.

4.3 Deterioration of MICP-treated slope soil under acid rain

It is evident that the corrosion of $CaCO_3$ is the deterioration mode of MICP-treated soils under the exposure of acid rain, which led to the loss of soil and UCS. Figure 11 presents the compilation of all soil loss measurements obtained versus the corrosion of $CaCO_3$ (as the percentage). From Fig. 11, it is found that the soil loss, with the corrosion of $CaCO_3$, can be fairly evaluated by linear relationships. In addition, the effect of cementation level is clearly witnessed from the plot, which further verifies the discussion made in previous section. Figure 12 presents the compilation of test data, i.e., UCS plotted against the corrosion of calcium carbonate. The

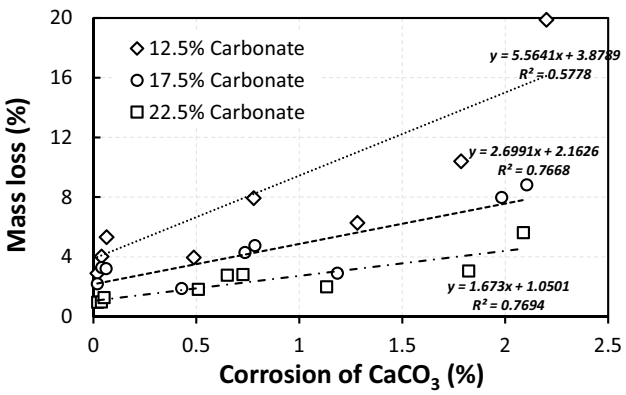

Fig. 11 The compilation of mass loss measurements (of all the 27 number of MICP treated specimens tested) versus corrosion of $CaCO_3$

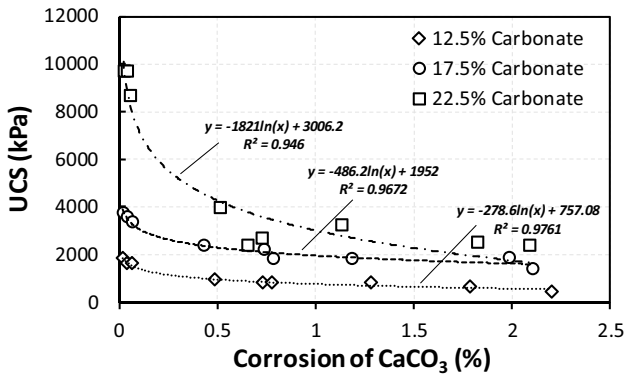

Fig. 12 The compilation of UCS measurements (of all the 27 number of MICP treated specimens tested) against corrosion of $CaCO_3$

results indicate that the UCS of the specimens exponentially decrease with the increase in corrosion of $CaCO_3$ for all the levels of cementation. The exponential tendency in decrease can be explained by the decay of matrix support. During the MICP treatment, the cementation begins at particle contact, increasing the strength gradually (progression of contact cementation). With the increasing treatment, the $CaCO_3$ crystals start to grow within the pore spaces (pore filling), sometimes bridging the particles (DeJong et al. 2010; Lin et al. 2016), which leads to rapid increase in strength at latter stage. The exponential progression of UCS in MICP-treated soils was evidenced in many previous studies (van Paassen et al. 2010; Gowthaman et al. 2019b; Choi et al. 2020). The plots observed herein (Fig. 12) demonstrate that the UCS follows relatively the similar path for the decrease during corrosion. It is worth mentioning that for a same corrosion value of $CaCO_3$, the specimens treated to higher cementation level exhibit lesser soil loss (Fig. 11) and persist higher in UCS (Fig. 12).

4.4 Limitations and future research

There are few limitations in the current work; therefore, further studies are still needed. Despite many useful findings, entire responses of the MICP-treated slope surface were not captured herein. Notably, the topography of the slope, one of the important factors determining processes such as rill, infiltration, and associated soil loss (Guerra et al. 2017; Zhang et al. 2018), was not evaluated. Therefore, an extensive model study considering slope aspects (such as gradient, texture and length) is recommended under the simulated acid rainfall to evaluate the effects of flow characteristics (runoff-infiltration) on longevity of the treatment. Besides, the properties such as grain size distribution, organic matter content, and soil mineralogy can possibly influence the long-term performance of MICP treatment (Mortensen et al. 2011; Cheng et al. 2016; Chung et al. 2020); thus, their effects under simulated acid rain are worthwhile to investigate in the future. Moreover, the study revealed that the acid rain deteriorates the MICP-treated slope surface under the prolonged exposure; therefore, an occasional re-treatment (implementing bacteria and rounds of cementation media) may be necessary to recover the $CaCO_3$ bridging between soil particles and to extend the performance of the slope cover. Therefore, an analysis on the re-treatment efficiency to the surface configuration is also recommended prior to real field applications.

5 Conclusions

MICP technology is an emerging and environmentally friendly alternative for stabilizing slope surface. In this work, an experimental program was conducted to evaluate the durability responses of MICP treatment slope soil under the exposure of acid rain. From the results, the following conclusions were obtained.

The corrosion of $CaCO_3$ was found to be the deterioration mode of MICP treatment, and the corrosion rate depended mainly on the pH conditions of acid rain. Lower pH conditions resulted in higher rates of corrosion. The intensity of acid rain was also found to have considerable impact in corrosion rate. High delivery rate (100 mm/h) led the acid rain solution to have less contact time within the specimen, which resulted in less reaction with $CaCO_3$. Low rate in acid rain delivery (20 mm/h) was more detrimental, which enabled increased reaction with carbonates, leading to severe damage in treatment.

Dissolution of $CaCO_3$ bonds at particle contacts led to the disaggregation of soil particles and loss of UCS, indicating that the MICP-treated slope soil is less durable under the exposure of acid rain. However, the study has demonstrated that the level of cementation greatly determines the durability of the MICP-treated soil. The higher the cementation level, the lower the loss of mass and UCS, enhancing the longevity of the treatment. For instance, under the supply of acid rain equivalent to the precipitation of 15 years, the observed soil loss was up to 19.9% for the specimens treated to 12.5% $CaCO_3$, whereas the evaluated losses were up to 8.8% and 5.6% for the specimens treated to 17.5% and 22.5% $CaCO_3$, respectively. SEM analysis further confirmed that the dissolution of bonds was achieved with shorter exposure for specimens cemented to lower level. The analysis showed that the soil loss, with the corrosion of $CaCO_3$, can be fairly evaluated by linear relationships, and UCS of the specimens exponentially decreases with the increase in corrosion of $CaCO_3$. Overall, this study suggests that the slope surface needs to be cemented to higher levels of $CaCO_3$ in order to enhance the durability and effective performance of MICP slope cover. The findings of this study would be

highly beneficial to extend the understanding on durability responses and to design an effective MICP treatments/re-treatments.

Electronic supplementary material The online version of this article (https://doi.org/10.1007/s11368-021-02997-w) contains supplementary material, which is available to authorized users.

Acknowledgements The authors would appreciate Hokkaido Regional Head Office, East Nippon Expressway Company Limited, Sapporo, Hokkaido, Japan, for the collaboration and supports provided during the field work.

Data availability All the experimental data that support the findings of this study are available from the corresponding author upon reasonable request through email.

Declarations

Competing interests The authors declare no competing interests.

References

Achal V, Mukherjee A (2015) A review of microbial precipitation for sustainable construction. Constr Build Mater 93:1224–1235. https://doi.org/10.1016/j.conbuildmat.2015.04.051

ASTM (2017) Standard practice for classification of soils for engineering purposes (Unified Soil Classification System). American Society for Testing and Materials, West Conshohocken, PA

Bakhshipour Z, Asadi A, Huat BBK et al (2016) Effect of acid rain on geotechnical properties of residual soils. Soils Found 56:1008–1020. https://doi.org/10.1016/j.sandf.2016.11.006

Bao R, Li J, Li L, et al (2017) Effect of microbial-induced calcite precipitation on surface erosion and scour of granular soils proof of concept. J Transp Res Board 2657:10–18. https://doi.org/10.3141/2657-02

Basu A, Ram BK, Nanda NK, Nayak SS (2020) Deterioration of shear strength parameters of limestone joints under simulated acid rain condition. Int J Rock Mech Min Sci 135 104508. https://doi.org/10.1016/j.ijrmms.2020.104508

Burbank M, Weaver T, Lewis R et al (2013) Geotechnical tests of sands following bioinduced calcite precipitation catalyzed by indigenous bacteria. J Geotech Geoenvironmental Eng 139:928–936. https://doi.org/10.1061/(ASCE)GT.1943-5606.0000781

Chen X, Achal V (2020) Effect of simulated acid rain on the stability of calcium carbonate immobilized by microbial carbonate precipitation. J Environ Manage 264 110419. https://doi.org/10.1016/j.jenvman.2020.110419

Cheng L, Cord-Ruwisch R (2014) Upscaling effects of soil improvement by microbially induced calcite precipitation by surface percolation. Geomicrobiol J 31:396–406. https://doi.org/10.1080/01490451.2013.836579

Cheng L, Cord-Ruwisch R, Shahin MA (2013) Cementation of sand soil by microbially induced calcite precipitation at various degrees of saturation. Can Geotech J 50:81–90. https://doi.org/10.1139/cgj-2012-0023

Cheng L, Shahin MA, Mujah D (2016) Influence of key environmental conditions on microbially induced cementation for soil stabilization. J Geotech Geoenvironmental Eng 143:04016083. https://doi.org/10.1061/(asce)gt.1943-5606.0001586

Choi SG, Chang I, Lee M et al (2020) Review on geotechnical engineering properties of sands treated by microbially induced calcium carbonate precipitation (MICP) and biopolymers. Constr Build Mater 246 118415. https://doi.org/10.1016/j.conbuildmat.2020.118415

Chung H, Kim SH, Nam K (2020) Application of microbially induced calcite precipitation to prevent soil loss by rainfall: effect of particle size and organic matter content. J Soils Sediments. https://doi.org/10.1007/s11368-020-02757-2

Cui MJ, Zheng JJ, Zhang RJ et al (2017) Influence of cementation level on the strength behaviour of bio-cemented sand. Acta Geotech 12:971–986. https://doi.org/10.1007/s11440-017-0574-9

DeJong JT, Mortensen BM, Martinez BC, Nelson DC (2010) Bio-mediated soil improvement. Ecol Eng 36:197–210. https://doi.org/10.1016/j.ecoleng.2008.12.029

Eyssautier-Chuine S, Marin B, Thomachot-Schneider C et al (2016) Simulation of acid rain weathering effect on natural and artificial carbonate stones. Environ Earth Sci 75:748. https://doi.org/10.1007/s12665-016-5555-z

Feng K, Montoya BM (2016) Influence of confinement and cementation level on the behavior of microbial-induced calcite precipitated sands under monotonic drained loading. J Geotech Geoenvironmental Eng 142:04015057. https://doi.org/10.1061/(ASCE)GT.1943-5606.0001379

Feng K, Montoya BM (2017) Quantifying level of microbial-induced cementation for cyclically loaded sand. J Geotech Geoenvironmental Eng 143:06017005. https://doi.org/10.1061/(ASCE)GT.1943-5606.0001682

Fukue M, Nakamura T, Kato Y (1999) Cementation of soils due to calcium carbonate. Soils Found 39:55–64. https://doi.org/10.3208/sandf.39.6_55

Gowthaman S, Iki T, Nakashima K et al (2019a) Feasibility study for slope soil stabilization by microbial induced carbonate precipitation (MICP) using indigenous bacteria isolated from cold subarctic region. SN Appl Sci 1:1480. https://doi.org/10.1007/s42452-019-1508-y

Gowthaman S, Mitsuyama S, Nakashima K et al (2019b) Biogeotechnical approach for slope soil stabilization using locally isolated bacteria and inexpensive low-grade chemicals: a feasibility study on Hokkaido expressway soil, Japan. Soils Found 59:484–499. https://doi.org/10.1016/j.sandf.2018.12.010

Gowthaman S, Nakashima K, Kawasaki S (2020) Freeze-thaw durability and shear responses of cemented slope soil treated by microbial induced carbonate precipitation. Soils Found 60:840–855. https://doi.org/10.1016/j.sandf.2020.05.012

Grennfelt P, Engleryd A, Forsius M et al (2020) Acid rain and air pollution: 50 years of progress in environmental science and policy. Ambio 49:849–864. https://doi.org/10.1007/s13280-019-01244-4

Guerra AJT, Fullen MA, Jorge M.D.CO et al (2017) Slope processes, mass movement and soil erosion: a review. Pedosphere 27:27–41. https://doi.org/10.1016/S1002-0160(17)60294-7

Harden CP, Scruggs PD (2003) Infiltration on mountain slopes: a comparison of three environments. Geomorphology 55:5–24. https://doi.org/10.1016/S0169-555X(03)00129-6

JGS (2012) Japanese standards and explanations of geotechnical and geoenvironmental investigation methods (3431–2012). Japanese Geotechnical Society, Tokyo, pp 426–432

Jiang N-J, Tang C-S, Yin L-Y et al (2019) Applicability of microbial calcification method for sandy-slope surface erosion control. J Mater Civ Eng 31:04019250. https://doi.org/10.1061/(ASCE)MT.1943-5533.0002897

Kamon M, Ying C, Katsumi T (1997) Effect of acid rain on physico-chemical and engineering properties of soils. Soils Found 37:23–32. https://doi.org/10.3208/sandf.37.4_23

Li C, Wang Y, Zhou T et al (2019) Sulfate acid corrosion mechanism of biogeomaterial based on MICP technology. J Mater Civ Eng 31:1–11. https://doi.org/10.1061/(ASCE)MT.1943-5533.0002695

Lin H, Suleiman MT, Brown DG, Kavazanjian E (2016) Mechanical behavior of sands treated by microbially induced carbonate precipitation. J Geotech Geoenvironmental Eng 142:04015066–1–4015113. https://doi.org/10.1061/(ASCE)GT.1943-5606.0001383

Liu KW, Jiang NJ, Qin JD et al (2020) An experimental study of mitigating coastal sand dune erosion by microbial- and enzymatic-induced carbonate precipitation. Acta Geotech 0123456789. https://doi.org/10.1007/s11440-020-01046-z

Liu S, Wen K, Armwood C et al (2019) Enhancement of MICP-treated sandy soils against environmental deterioration. J Mater Civ Eng 31:1–13. https://doi.org/10.1061/(ASCE)MT.1943-5533.0002959

Martinez BC, DeJong JT, Ginn TR et al (2013) Experimental optimization of microbial-induced carbonate precipitation for soil improvement. J Geotech Geoenvironmental Eng 139:587–598. https://doi.org/10.1061/(ASCE)GT.1943-5606.0000787

Montoya BM, Jong De JT (2015) Stress-strain behavior of sands cemented by microbially induced calcite precipitation J Geotech Geoenvironmental Eng 141. https://doi.org/10.1061/(ASCE)GT.1943-5606.0001302

Mortensen BM, Haber MJ, Dejong JT et al (2011) Effects of environmental factors on microbial induced calcium carbonate precipitation. J Appl Microbiol 111:338–349. https://doi.org/10.1111/j.1365-2672.2011.05065.x

Muntohar AS, Liao HJ (2010) Rainfall infiltration: infinite slope model for landslides triggering by rainstorm. Nat Hazards 54:967–984. https://doi.org/10.1007/s11069-010-9518-5

Nafisi A, Montoya BM, Evans TM (2020) Shear strength envelopes of biocemented sands with varying particle size and cementation level. J Geotech Geoenvironmental Eng 146:04020002. https://doi.org/10.1061/(ASCE)GT.1943-5606.0002201

Omoregie AI, Palombo EA, Ong DEL, Nissom PM (2019) Biocementation of sand by *Sporosarcina pasteurii* strain and technical-grade cementation reagents through surface percolation treatment method. Constr Build Mater 228 116828. https://doi.org/10.1016/j.conbuildmat.2019.116828

Salifu E, MacLachlan E, Iyer KR et al (2016) Application of microbially induced calcite precipitation in erosion mitigation and stabilisation of sandy soil foreshore slopes: a preliminary investigation. Eng Geol 201:96–105. https://doi.org/10.1016/j.enggeo.2015.12.027

Tang CS, Yin L, yang, Jiang NJ et al (2020) Factors affecting the performance of microbial-induced carbonate precipitation (MICP) treated soil: a review. Environ Earth Sci 79:94. https://doi.org/10.1007/s12665-020-8840-9

Teir S, Eloneva S, Fogelholm CJ, Zevenhoven R (2006) Stability of calcium carbonate and magnesium carbonate in rainwater and nitric acid solutions. Energy Convers Manag 47:3059–3068. https://doi.org/10.1016/j.enconman.2006.03.021

van Paassen LA, Ghose R, van der Linden TJM et al (2010) Quantifying biomediated ground improvement by ureolysis: large-scale biogrout experiment. J Geotech Geoenvironmental Eng 136:1721–1728. https://doi.org/10.1061/(ASCE)GT.1943-5606.0000382

Wei MW, Xie JH, Zhang H, Li JL (2019) Bond-slip behaviors of BFRP-to-concrete interfaces exposed to wet/dry cycles in chloride environment. Compos Struct 219:185–193. https://doi.org/10.1016/j.compstruct.2019.03.049

Xie S, Qi L, Zhou D (2004) Investigation of the effects of acid rain on the deterioration of cement concrete using accelerated tests established in laboratory. Atmos Environ 38:4457–4466. https://doi.org/10.1016/j.atmosenv.2004.05.017

Zhang C, Li F, Lv J (2017) Morphology and formation mechanism in precipitation of calcite induced by *Curvibacter lanceolatus* strain HJ-1. J Cryst Growth 478:96–101. https://doi.org/10.1016/j.jcrysgro.2017.08.019

Zhang X, Hu M, Guo X et al (2018) Effects of topographic factors on runoff and soil loss in Southwest China. CATENA 160:394–402. https://doi.org/10.1016/j.catena.2017.10.013